Increase lifespan with a cell management algorithm in electric energy storage systems

Christophe Savard , Pascal Venet , Laurent Piétrac , Éric Niel and Ali Sari,
Univ Lyon, École Centrale Lyon, INSA Lyon, Université Claude Bernard Lyon 1,
CNRS, Ampère UMR 5005, 69100 Lyon, France

***Abstract*—This paper presents a different way to manage batteries composed by association of basic and redundancy cells. This is an algorithm adapting the internal configuration according to the state of charge of each cell in order to reduce cycling aging effects that cells undergo during normal operation. The lithium-ion pack reliability is summarized in this article before a presentation of simulation results. It is demonstrated that with the introduced cell management scheme, the useful remaining lifespan of the battery can be increased. As a result, adding redundant cells to increase lifespan becomes economically viable.**

***Index Terms*—Battery model, aging parameters, lifespan, reconfiguration**

I. Introduction

This article presents a particular point of a global work related to the search for an effective architecture improving performance in terms of lifespan, reliability and operative dependability for electric energy storage systems (EESS). It has been found appropriate to split this part of this work because, whatever the architecture, this aspect can be implemented for improving EESS performances.

EESS are used both from battery-household appliances to complex systems in electric mobility and for stationary storage. EESS are characterized not only by their current and voltage but also by their announced lifespan. Often this duration is expressed by manufacturers in cycles, including calendar and cycling aging [1]. The cycles include the processing time: the discharging phase and the charging phase. To improve lifespan, a lot of solutions are proposed [2]. Some of them are based on internal reconfiguration [3], [4]. [5] looked at a solution which would save resources of the batteries by an internal reconfiguration and an optimized management. By resources, it is meant all associated cells within EESS. Switches, the Battery Management System (BMS) and possible systems for other functions (such as dissipative balancing circuits or measurement of physical parameters) are considered here as additional elements. That is to say that we can refrain from taking into account the possible failures of these additional elements in this article.

Consider that cells operate in maturity phase in terms of reliability. Also consider that all associated cells in a battery follow the same reliability laws, expressed by their instantaneous failure rate λ_{cell}. Then, reliability $R_{cell}(t)$ follows an exponential law reminded in equation (1). Indeed, consider for example the switches. They have instantaneous failure rate such as their probability of default remains lower than the cells, even solicited in full production. Cells have announced lifespan generally between 500 and 2000 cycles [6], [7]. The switches consist of MOSFET or IGBT, whose instantaneous failure rate fluctuates around 10 FIT (Failure in Time, 10^{-9}default per hour). Without considering the effects of temperature, even if the transistor was requested a thousand times during a cycle and by admitting that its probability of failure was proportional to its requests, it would be 100 times more reliable than the cell.

$$R(t) = e^{-\lambda_{cell}.t} \tag{1}$$

This study does not examine the cell chemical or technical inherent improvement but focuses on seeking ways to more relevant use them.

II. Resource use

A single electrical energy storage element, namely a cell, is only able to provide its nominal current at a preset voltage. The delivered voltage, in order to a few volts for a cell, is not enough to provide electric power devices [8]. Thus the EESS consists of cells connected in series to increase voltage and connected in parallel to increase the output current. Figure 1 shows the principle of this cell association in EESS whose electrical properties are then adjusted to the needs of the source by a DC / DC converter (which is outside the study scope) [9]. The switch S_{ij} can disconnect the cell $Cell_{ij}$ from the remainder of the battery.

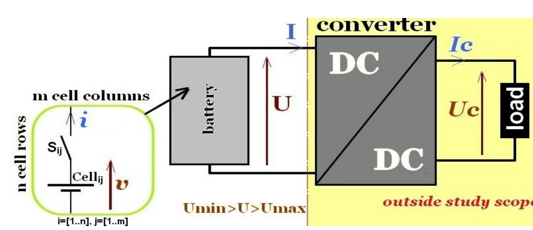

Fig. 1. A battery include a number of basic cells

However, if a cell has an instantaneous failure rate of λ_{cell} and battery associates for instance in parallel two strings of four cells, the battery failure rate will be worth $8\lambda_{cell}$. Accordingly, the mean time to failure (MTTF) of the battery will be 8 times smaller than for a single cell. Because, in maturity phase, reliability follows the exponential low, as shown by equation (1), the MTTF is given by equation (2). Indeed, the eight cells must all be operational so that the battery is also operational. Thereby, its MTTF is worth one eighth of that of a single cell.

$$MTTF_{cell} = \int_{t=0}^{+\infty} R_{cell}(t).dt = \frac{1}{\lambda_{cell}} \tag{2}$$

To improve the reliability of the battery, it is then necessary to employ redundant cells, for instance as shown in Figure 2 by adding, in this case, a third string of four cells in passive redundancy. With an instantaneous failure rate $\lambda_{cell} = 10^{-3}\ default/cycle$, the battery MTTF falls to 125 cycles without redundancy (a single-cell battery reach 1000 cycles). General formula for passive redundancy $R_{pas}\left(t\right)$ is depict in equation (3), when R_{cell} is the reliability of one element, x is the number of basic cells and y the total, as show in Figure 3. With redundancy, this example MTTF worth 208 cycles. The addition of a second string of redundancy further improves this MTTF to 271 cycles. Nevertheless, a multi-cell battery is always less reliable than a single cell battery. Double the number of cells hoping to double the reliability is only true for a battery consisting of a single cell [10]. Regardless of the number of associated redundant cells, add it improve reliability. The swapping between the basic and redundant elements are enabled through switches. Redundancy is not implemented today in marketed batteries because the addition of a P percent of redundancy does not bring an improvement in $P\%$ of the lifespan.

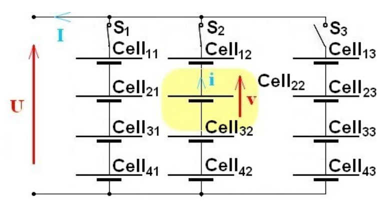

Fig. 2. First theoretical study structure

$$R_{pas}\left(t\right) = R_{cell}^{x}.\left(1 + \sum_{i=1}^{y-x}\left(\frac{(1-R_{cell})^{i}}{i!}\right).\prod_{j=1}^{i}(x+j-1)\right) \tag{3}$$

What is more, the electrical characteristics of the associated cells in series and in parallel inside a battery are not all identical. Intrinsically, disparities come from the conditions of manufacturing of each cell, particularly with regard to manufacturing tolerances [11]. In use, they come from the conditions of use, including the maximum current that cells had to provide. Thus, inside a battery, various strategies can be deployed to balance the electrical characteristics. For instance, the state of charge (SoC) of cells may be equalized [12]. To permit balancing between some associated cell, it is necessary to add the switches in order to create appropriate paths for the currents of each cell. BMS is responsible for managing the balance between electrical characteristics [13]. To date, inserted switches are only used for balancing the cells. But having a matrix structure with rows and columns of cells, connected by switches can also allow dynamic reconfigurations for a better resource using, by allowing a different internal balancing.

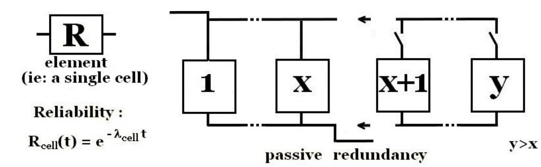

Fig. 3. Cells associated in passive redundancy, general case

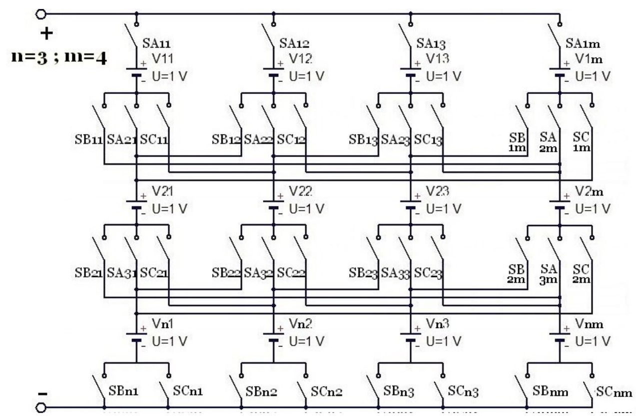

Fig. 4. C3C architecture, example with three rows and four columns

In order to increase the number of degrees of freedom allowing a reconfiguration, a new structure to link cells together is proposed: the C3C architecture [5]. This involves allowing the outgoing flow of one cell to join three further cells downstream as upstream (in charging as in discharging phase). An example of a C3C architecture is shown in Figure 4. It has been demonstrated that the reliability of a C3C architecture is the same as a parallel-series architecture (PS) when redundancy in limited to one column [10], [5]. Depending on the n rows and m columns of cells, the reliability $R_{PS}(t)$ of the PS architecture is expressed by the equation (4). $MTTF_{PS}$ of such a structure of cells in mature phase is described by the equation (5).

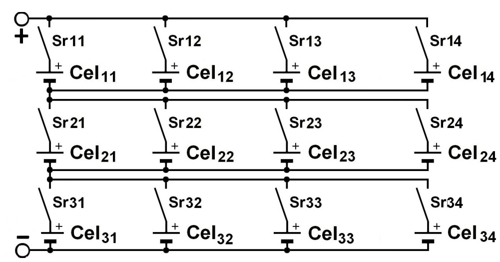

Fig. 5. PS architecture, example with three rows and four columns

$$R_{PS}(t) = e^{-n.(m-1).\lambda_{cell}.t}.(1+\lambda_{cell}.t)^{n.(m-1)} \tag{4}$$

$$MTTF_{PS} = \sum_{k=0}^{n.(m-1)} \binom{n.(m-1)}{k} \frac{1}{n.(m-1)^k.\lambda_{cell}} \quad (5)$$

This architecture is associate with a different principle for using resources. Indeed, in a conventional PS architecture, when a cell should fail, it is isolated and replaced by the redundant cell. Failure appears when a cell is no longer able to store sufficient energy. The C3C obeys different principle. Since on each row the structure has an extra cell to the needs, this latter is not let in stand-by until cell failure but is used as any of the other cells while keeping one cell at rest. So, this dynamic operation modifies the conditions of exploitation of other resources. It seems appropriate to examine whether that simple change in the way of using resources improves or not the lifespan of the battery, whatever the architecture.

Part three presents operating principles of the internal resource management algorithm. Then, main factors which contribute to cell aging are remind by briefly presenting the developed electrical model. In the fifth part, operative dependability and life expectancy for a PS architecture running in a classical way and operating with our algorithm are compared.

III. Developed algorithm

In order to demonstrate the operation of the algorithm, consider another architecture: a set of cells connected in parallel, as shown in Figure 6. The following example consider a structure of four parallel columns, which represents a row of a PS architecture. One cell provides redundancy. This theoretical assembly is thus empowered to provide three times the power of a single cell. Cell electrical characteristics - internal equivalent series resistance (ESR), nominal capacity - are not identical. Similarly, the structure regards to be recharged under its nominal current, that is to say $-3.i$, with i the cell nominal current. In this example, cells are not used beyond their nominal current.

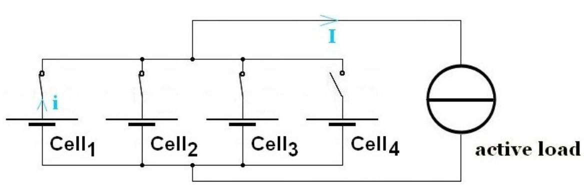

Fig. 6. Demonstrate scheme with three basic and one redundant cells

To ensure that the proposed architecture meets the requirements of the external load specs, it is necessary to have at least three functional cells. So, in other words, their SoC does not equal to zero. At first, the four cells are fully charged: $SoC(t = 0) = 1$. Suppose they are subject to highly variable behavior when they are solicited. Suppose too, to meet the specifications, they react differently in terms of depth of discharge. We take readings the cell state of charge at each measurement step. In this caricaturing example, between each measurement, we consider respectively 30%, 25%, 20% and 15% SoC decease.

By simulating this system operation, using the fourth cell in conventional redundancy, the amount of charge in each cell evolve as depict in Table I. After, in step 3.3, $Cell_1$ is empty. It is isolated and the spare cell supplant it. When a second cell becomes empty, the battery is not along able to meet requirements (not able to provide a current of $3i$). Lifespan improvement is therefore only $\frac{4}{3.3}$ (ie +21%) with a 33% addition of cells.

TABLE I
SoC evolution in Figure 6 structure, without algorithm

Step	$Cell_1$	$Cell_2$	$Cell_3$	$Cell_4$
0	100	100	100	100
1	70	75	80	100
2	40	50	60	100
3	10	25	40	100
3.3	0	17	33	100
4	0	0	20	85

TABLE II
SoC evolution in Figure 6 structure, with management algorithm

Step	$Cell_1$	$Cell_2$	$Cell_3$	$Cell_4$	active cells
0	100	100	100	100	1 2 3
1	70	75	80	100	2 3 4
2	70	50	60	85	1 3 4
3	40	50	40	70	1 2 4
4	10	25	40	55	2 3 4
5	10	0	20	40	1 3 4
5.3	0	0	13	35	-

Now, try to postponement this deadline. The electrical characteristics of a battery, in particular SoC are identified and estimated, for example by Kalman filters [14] and processed by the BMS [15]. This means that cell with the minimum SoC (maximum in a charging phase) among the four cells can be determined.

Otherwise, with our resource management algorithm, we start with the same configuration ($Cell_1$, $Cell_2$ and $Cell_3$ are ON). All cells are fully charged, as shown in the first row in Table II. The algorithm (1) is applied. It consists of detecting in a row, for a PS architecture, the weakest cell (that is to say the least charged in discharging mode) and to place it at rest while activating the one previously placed at rest. Then, after calculation, at the first step, it seems that $Cell_1$ is the most depleted. So, it is substituted by spare $Cell_4$. The $Cell_1$ becomes since that the redundant cell. In this way, redundancy is dynamically managed. If, for a cell, the time to return to thermodynamic equilibrium is less than the time during which it will be put on stand-by, it may still be considered in passive redundancy. As a result, at each measurement step, the more discharged cell swaps with the spare cell. When several cells have the same minimal SoC, favor the cell that has the least been put to use, as is the case after three steps in this example.

Hence, the battery has a better operative dependability, since it was able to deliver its maximum current during 5.3 measurement steps instead of only 4 if the redundant cell was only activated at the first failure.

Algorithm 1 Optimization algorithm for a PS architecture

```
Battery : n rows and m columns
Initial state : all cells actives by row, except one (k)
For i=1:n
  Detect weakeast cell (j)
  if j<>k then
    Active cell j
    Rest cell k
  end{if}
end{for}
Final state : all cells actives by row, except the weakest

Weakest cell in a row :
  in charging mode : cell with SoC max
  in discharging mode : cell with SoC min
```

IV. Cell aging factors

This algorithm has been implemented in a Matlab® [12] simulation for which a specific cell model is developed. It is describe in detail in [16]. As a matter of fact, since controlling the evolution of each parameter cell is needed to monitor developments, the standard model don't suit. The model is based on characteristic equation binding the SoC and open-circuit voltage measurement, and the cell expected lifetime subjected to specified discharge-recharge cycles. It considers three factors aggravating to aging: temperature, depth of discharge and current value, based on analysis and research already conducted on aging batteries [17]. The aging takes place in two complementary ways: calendar and cycling manners. The calendar aging results internal phenomena [18] and localized production of gas particles [19]. These phenomena contribute to the reduction of the SoC as well as another cell characteristic parameter: the state of health (SoH).

The state of health reflects the fact that the maximum capacity of a battery decreases with time. The more a battery ages and the less it is able to store energy [20]. SoH is a direct image of aging. Usually, when it falls below 80%, which means that the battery is no longer able to store 80% of its initial capacity, the battery is considered at the end of life, as it is advise in the $ISO - 12405 - 2 :\ 2012$ standard (Electrically propelled road vehicles, test specification for lithium-ion traction battery packs and systems, high-energy applications). This value is noted S_{lim} in this paper.

In optimal conditions, the advertised lifetime (noted Lf) is used to define when SoH reach down to S_{lim}. Three aggravation parameters are added, respectively A_i, A_d and A_t, related to the extracted current in the k^{th} cycle and indexed $A^{(k)}$, the depth of discharge and the temperature. For an optimal use, each parameter value to 1. Together, they help reduce the lifespan from $S_0 = 1$. SoH follows the law 6.

$$SoH\left(\Upsilon\right) = S_0 - \left(1 - S_{lim}\right) . \sum_{k=1}^{\Upsilon} \left[\frac{A_i^{(k)} . A_d^{(k)} . A_t^{(k)}}{Lf} \right] \quad (6)$$

Thus, each cell does not age in the same way that another also because of intrinsic differences resulting from its realization [21]. The design involve in the disparity of electrical and chemical characteristics, particularly because of the manufacturing process, the quality of composition of the electrolyte, the quality of the seal, assembly and handling conditions on the production line and possible contamination of the constituent parts. The conditions of use also interfere greatly on maintaining electrical performances. Certain conditions of use penalize the life of batteries as over current. The environment that are used or stored batteries also influences the speed of aging, including operating temperature, maximum temperature of storage, mechanical stress and corrosive environment conditions. All of this occurs in the calendar and cyclic aging of a battery.

Primary parameters are taken into account in the model which is used to assemble any number of cells in rows and columns and to compare the results. Parameters such as initial ESR, initial temperature and maximal charge of each cell are defined randomly around an average value (more or less 10% around nominal value). The strength of this model consists in simulate any type of cell by extracting the parameters of the curve giving the evolution of the open circuit voltage in function of the state of charge.

V. Simulation results

Simulation consists in submitting the four-cells one-row structure of Figure 6 to a continuous cycling, as depict in Figure 7, including same duration three phases. In first, cells are discharged by removing a significant portion of their initial nominal capacity (70% of the initial capacity). Then cells are charged again during the same period. Finally, the cells leave at rest for the same time.

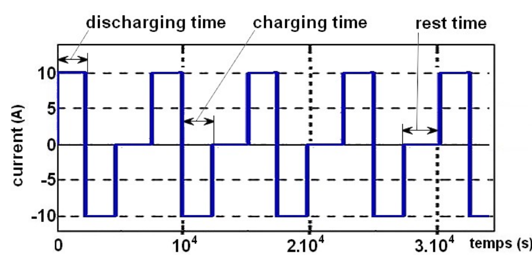

Fig. 7. Cycling test

The relaxation phase (no current flowing) is used to estimate the electrical parameters such as SoC and SoH, knowing that they will also be used as a weight parameter in optimizations related to the C3C structure. This point is not the subject of this paper. Since each phase lasts 2500 seconds, a cycle takes 7500 seconds, that is a little more than two hours.

Simulation is performed in two passes. First, without failure other than the progressive aging of cells. In consequence, simulation stops when two cells are discharged or they both have a SoH less than the minimum of 80%. The first one having failed has been replaced by the redundant. Second, with a failure of the $Cell_2$ after a predefined time, close to three-fifths of the lifespan of a cell, that is default to 1000 cycles. A threshold of 10% in the SoC variation is chosen to allow commutation in this simulation. That is to say that swapping operates when the difference between the most and the less SoC is more than 0.1. To avoid a self-balancing, which could distort the results of simulations, cells are considered disconnected from each other during the relaxation phase. Note that in these simulations, cells can not be charged beyond their maximum capacity. It is consider that the BMS has the responsibility to manage the overflow potential energy when recharging the battery and that cells are recharged behind a CC-CV protocol (first charging with constant current, last with constant voltage). Similarly, the operation is only simulated with nominal current rating although with lower current cell ages less rapidly, as it was mentioned in the previous chapter.

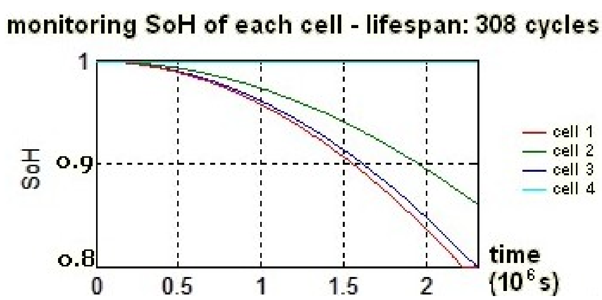

Fig. 8. SoH of the four cells with time, without algorithm, without failuree

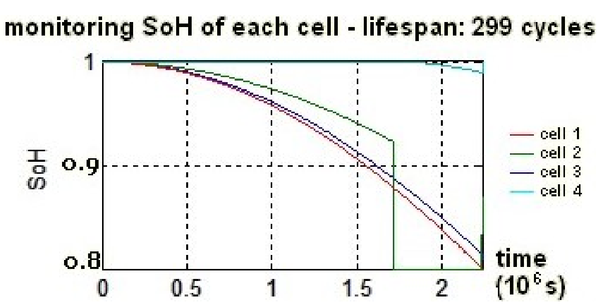

Fig. 9. SoH of the four cells with time, without algorithm, with $Cell_2$ failure

Figures 8 and 9 show a simulation carried out without using the resource management algorithm. Each cell is aging differently although strictly identical, apart from slight variations on initial conditions in maximum capacity and ESR. The $Cell_4$ ages only in a calendar way. This results in a decrease in SoH not visible on the cyan trace. As soon as it replaces $Cell_1$ in Figure 8 or $Cell_2$ in Figure 9, it begins to age cyclically. Figures 10 and 11 present exactly the same cells in processing but managed with the algorithm. Without a $Cell_2$ (green curve) forced failure (Figure 9), Figure 8 shows that $Cell_1$ (red) is the first whose SoH decreases to 0.8. It is then replaced by $Cell_4$ (cyan) which begins to age. The battery ceases to be functional when a second cell fails by aging: the $Cell_3$(blue). When $Cell_2$ prematurely fails (Figure 9), $Cell_1$ failure (red) causes battery failure.

A performance indicator is defined as the ratio between the lifespan of variants divided by the lifespan in a battery witch just use $(m-1)$ cells in a conventional way, as describe in equation (7). Variants consist in using m^{th} cell in redundancy or in using all cells with the algorithm. This indicator is tested with a large number of simulations on different battery structures (various numbers of columns) in the PS and C3C architectures by keeping $n = 2$. In Figure 12, the orange curve shows results for PS with algorithm and the yellow for using algorithm in a C3C architecture. The number of cells implanted in the battery as defined by the equation (8), is represented in green, to compare. Finally, the indicator obtained by classically using redundancy in PS architecture is draw by the blue curve.

$$performance = \frac{lifespan\ of\ variant}{lifespan\ of\ \ (m-1)\ cell\ battery} \quad (7)$$

$$cost = \frac{number\ of\ redundant\ cells}{number\ of\ basic\ cells + number\ of\ redundant\ cells} \quad (8)$$

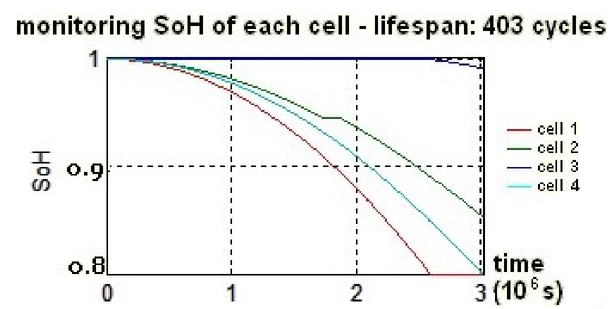

Fig. 10. SoH of the four cells with time, with algorithm, without failure

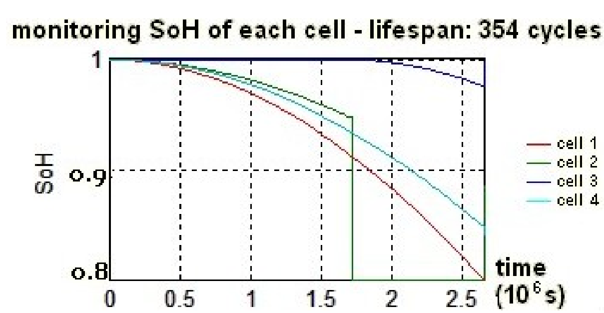

Fig. 11. SoH of the four cells with time, with algorithm, with $Cell_2$ failuree

From this analysis, it appears that the solutions using the algorithm present an improvement in the operative dependability that balances the additional cost associated with the presence of redundant cells. For its part, the addition of a cell column in redundancy improves the operating availability but in a lesser way. Moreover, this improvement in operative dependability, ie $+12\%$ (blue line in Figure (12)) when $m = 4$ does not compensate the additional cost, witch is equal to $\frac{1}{m-1}$: $+33\%$. On the other hand, optimizing the cells according to their SoC allows a gain in lifespan of an amount close to the number of redundant cells. Indeed, the cost green curve in the figure describes the ratio between the number of total cells (including redundancy) on the number of active cells. By adding redundant cells in a matrix structure battery, the lifespan is not increased proportionally to the number of spares cells. With the optimization algorithm, it is possible to increase the lifespan by making the number of additional cells profitable.

Fig. 12. Comparative performances on algorithm improvement, with $n = 2$

VI. Conclusions

As expected, managing energy by choosing among the available cells those that are most relevant, increase the length of time a battery is available. This results in a reduction of the aging of the internal cells aging. By limiting redundancy to only one cell per row in a matrix architecture of EESS, we have demonstrated in this paper that a parallel combination of cells could stay longer operational. A series association of these structures may see its lifetime increase in the same proportions. The redundancy extra cost is offset by operative dependability improvement, that is to say a longer lifespan. Optimization by other criteria than SoCs (maximum capacity, SoH, temperature) should be sought in such a way that the improvement of the operative dependability is economically profitable. Through the use of an algorithm which dynamically define the idle cell, the use of conventional redundancy in a multi-cell battery can be considered as an economically viable solution. It makes it possible to increase the lifespan of a battery at least in proportion to the quantity of additional cells. By resorting to another optimization criterion that the SoC, focused on slowing the aging of cells, it must be possible to further improve this lifespan.

References

[1] A. Wu, D. Wu, and C. Wang, "Failure mechanism due to aging effects in lithium-ion batteries," in *2015 IEEE International Telecommunications Energy Conference (INTELEC)*, Oct. 2015, pp. 1–6.

[2] Y. Kim, S. Park, Y. Wang, Q. Xie, N.Chang, M. Poncino, and M. Pedram, "Balanced reconfiguration of storage banks in a hybrid electrical energy storage system," in *2011 IEEE/ACM International Conference on Computer-Aided Design (ICCAD), San Jose, CA*, 2011, pp. 624–631.

[3] H. Kim and K. G. Shin, "Desa: Dependable, efficient, scalable architecture for management of large-scale batteries," *IEEE Transactions on Industrial Informatics*, vol. 8, no. 2, pp. 406–417, May 2012.

[4] F. Jin and K. G. Shin, "Pack sizing and reconfiguration for management of large-scale batteries," *Cyber-Physical Systems (ICCPS), 2012 IEEE/ACM Third International Conference on, Beijing*, pp. 138–147, 2012.

[5] C.Savard, A.Sari, and al., "C-3c: a sstructure for high reliability with minimal redundancy for batteries," in *2016 ICIT International Congress of Industrial Technology, Taipei*, Mar. 2016.

[6] N. Mukherjee and D. Strickland, "Second life battery energy storage systems: Converter topology and redundancy selection," in *Power Electronics, Machines and Drives (PEMD 2014), 7th IET International Conference on, Manchester*, 2014, pp. 1–6.

[7] R. Xiong and el., "Modeling for lithium-ion battery used in electric vehicles," *Procedia Engineering*, no. 15, pp. 2869–2874, 2011.

[8] Y. Ye and K. W. E. Cheng, "Modeling and analysis of seriesâĂŞparallel switched-capacitor voltage equalizer for battery/supercapacitor strings," *IEEE Journal of Emerging and Selected Topics in Power Electronics*, vol. 3, no. 4, pp. 977–983, Dec. 2015.

[9] N. Rizoug, G. Feld, B. Barbedette, and R. Sadoun, "Association of batteries and supercapacitors to supply a micro-hybrid vehicle," in *2011 IEEE Vehicle Power and Propulsion Conference, Chicago, IL*, 2011, pp. 1–6.

[10] C.Savard, E.Niel, and al., "Amelioration de la fiabilite des structures matricielles de batteries," in *Lambda-Mu 2016*, 2016.

[11] A. Devie, "Caractérisation de l'usage des batteries lithium-ion dans les véhicules électriques et hybrides. application à l'étude du vieillissement et de la fiabilité," Energie électrique, Université Claude Bernard - Lyon 1, november 2012, français.

[12] W. Huang and J. A. A. Qahouq, "Energy sharing control scheme for state-of-charge balancing of distributed battery energy storage system," *IEEE Transactions on Industrial Electronics*, vol. 62, no. 5, pp. 2764–2776, May 2015.

[13] E. Chemali, M. Preindl, P. Malysz, and A. Emadi, "Electrochemical and electrostatic energy storage and management systems for electric drive vehicles: State-of-the-art review and future trends," *IEEE Journal of Emerging and Selected Topics in Power Electronics*, vol. 4, no. 3, pp. 1117–1134, Sep. 2016.

[14] R. Xiong and al., "Online estimation of peak power capability of li-ion batteries in electric vehicles by a hardware-in-loop approach," *Energies*, pp. 1455–1469, 2012.

[15] C. Sinkaram and V. A. K. Rajakumar, "Modeling battery management system using the lithium-ion battery," in *2012 IEEE International Conference on Control System, Computing and Engineering (ICCSCE)*, 2012, pp. 50–55.

[16] C. Savard, "Amélioration de la fiabilité opérationnelle des systèmes de stockages de l'énergie électrique multicellulaires," Génie Électrique, INSA de Lyon, november 2017, french.

[17] E. Redondo-Iglesias, P. Venet, and S. Pelissier, "Measuring reversible and irreversible capacity losses on lithium-ion batteries," in *2016 IEEE Vehicle Power and Propulsion Conference (VPPC), Hangzhou*, 2016.

[18] R. Yazami, "The activation energy of self-discharge in anode and cathode for lithium-ion batteries," in *internal edition of Division of Engineering and Applied Sciences California Institute of Technology, Pasadena, CA*, 2012.

[19] S. Bourlot, P. Blanchard, and S. Robert, "Investigation of aging mechanisms of highpower li-ion cells used for hybrid electric vehicles," *Journal of Power Sources*, no. 196, pp. 6841–6846, 2011.

[20] J. Jespersen and al., "Capacity measurements of li-ion batteries using ac impedance spectroscopy," *World Electric Vehicle Journal*, vol. 3, pp. 0127–0133, 2009.

[21] S. Mahalakshmi and S. Datchanamoorthy, "Prediction of wireless sensor battery life," in *IEEE AUTOTESTCON, 2015, National Harbor, MD,*, 2015, pp. 138–145.